COPOLYMER MICELLES WITH POLYELECTROLYTE SHELL IN AQUEOUS MEDIA. A MEAN-FIELD STUDY

Karel JELÍNEK[1], Filip UHLÍK[2], Zuzana LIMPOUCHOVÁ[3], Pavel MATĚJÍČEK[4] and Karel PROCHÁZKA[5,*]

Department of Physical and Macromolecular Chemistry, Faculty of Science, Charles University, Albertov 6, 128 40 Prague 2, Czech Republic, e-mail: [1] charlie@vivien.natur.cuni.cz, [2] uhlik@natur.cuni.cz, [3] zl@vivien.natur.cuni.cz, [4] matej@vivien.natur.cuni.cz, [5] prochaz@vivien.natur.cuni.cz

Received December 20, 2005
Accepted February 10, 2006

Dedicated to our great friend and colleague Dr Marta Pacovská who passed away a year ago.

The multimolecular micelles formed by polystyrene-*block*-poly(methacrylic acid) (PS-PMA) copolymer and by hydrophobically modified PS-PMA copolymer with naphthalene and anthracene (PS-N-PMA-A) were studied by self-consistent field (SCF) calculations in aqueous media. The labeling with covalently bonded naphthalene between PS and PMA blocks and with anthracene at the free end of PMA blocks, which is suitable for experimental nonradiative excitation energy transfer (NRET) studies of PS-N-PMA-A micelles, modifies the structure of micellar shell. The study was aimed at understanding structure and behavior of micelles at different pH and ionic strength. The results show that the presence of hydrophobic tags has only a small influence on the overall structure of micelles but it strongly affects the distribution of PMA free ends. The hydrophobic labels (anthracenes) try to return into the shell and their certain fraction is localized close to the core/shell interface, which causes a fairly high NRET efficiency. The calculated and experimentally measured NRET efficiency were compared; their trends are reasonable at the semiquantitative level.

Keywords: Mean-field calculations; Copolymer micelles; Polyelectrolytes; Poly(methacrylic acid); Aqueous solutions; SCF calculations; Nanoparticles.

Polymeric micelles and related nanoparticles soluble in aqueous media have been studied by a number of research groups in the past decade[1–4] due to their interesting potential applications, such as water pollutant removal or drug and gene delivery[5–9]. In this work we study the structure and behavior of micelles formed by polystyrene-*block*-poly(methacrylic acid) diblock copolymer (PS-PMA) and hydrophobically modified PS-N-PMA-A (PS-PMA block copolymer with incorporated hydrophobic tag naphthalene between PS and PMA blocks and anthracene at the ends of PMA blocks) in aqueous

Collect. Czech. Chem. Commun. 2006, Vol. 71, No. 5, pp. 756–768

doi:10.1135/cccc20060756

media by self-consistent field (SCF) calculations. The double tagging with naphthalene and anthracene is a suitable modification for fluorometric nonradiative energy transfer (NRET) studies allowing to compare experimental measurements with theoretically calculated data.

Symmetrical diblock copolymers in selective solvents (a good solvent for one block and a poor for the other) form spherical multimolecular micelles with compact core consisting of insoluble blocks and protective shell consisting of soluble blocks. The micelles are fairly monodisperse and coexist in equilibrium with a certain fraction of unimers. The solution of PS-PMA micelles in aqueous media cannot be prepared directly by dissolution of PS-PMA copolymer in water because the high-molecular-weight PS-PMA samples are water-insoluble. The micelles have to be prepared indirectly by dissolving the sample in a mixture of water and 1,4-dioxane (80 vol.%) where they form spontaneously. Then they are transferred into aqueous media by stepwise dialysis against solvents with increasing water content and finally against pure water. The equilibrium freezes at ca. 40–50% water content and thus the association number is not controlled by the composition of the final aqueous solvent. The PS cores are very compact in water and they are actually in the glassy state. The hydrophobic modification of copolymers by attaching the covalently bonded hydrophobic tags proceeds during the synthesis of single chains in organic solvents and does not require any modification in the method of micelle preparation.

While the behavior of PS cores is relatively simple, the behavior of PMA shells in aqueous media is fairly complex. PMA is a weak polyelectrolyte and its behavior depends on the degree of dissociation which is controlled by pH and ionic strength of the solution. The ionization of carboxylic groups of PMA is also affected by the presence of low dielectric permittivity components such as PS core and PMA segments. The attachment of hydrophobic tags at the ends of shell chains modifies the shell behavior because hydrophobic tags try to avoid unfavorable interactions with polar environment.

In our previous papers, we studied PS-PMA micelles by SCF and MC simulations in polar solvents where the dissociation of COOH groups of PMA could be neglected. Recently we extended our study to aqueous systems, which required introduction of long-range electrostatic interactions[10]. The hydrophobically modified systems PS-N-PMA and PS-N-PMA-A have not yet been studied in aqueous media. In this paper, we study the structure and behavior of PS-PMA and PS-N-PMA-A micelles in aqueous media by mean-field calculations based on the model of Scheutjens and Fleer[11].

MODEL

In the self-consistent field method developed by Scheutjens and Fleer, the polymer chain is modeled as the first-order Markov chain, which means that the position of a given segment is assumed to depend only on the position of the immediately preceding segment. The steps in all possible directions, including the reversal step, are allowed. The fundamentals of this method for weak polyelectrolytes as well as the computational scheme were described in numerous articles in detail[11–14].

Our model mimics polymeric micelles in very dilute solution where interactions between different micelles can be neglected and therefore the calculation for only a single micelle can be performed. The PS-PMA micelles are kinetically frozen in aqueous media, i.e., there is no exchange of chains between different micelles (the unimer concentration is practically zero). The association number is controlled by the solvent quality in which the micellization equilibrium freezes during the preparation of micelles. This means that it is constant in aqueous buffers, i.e., it does neither change with polymer concentration, nor with pH and ionic strength. Therefore we do not simulate spontaneous micellization, but we set the association number according to the experimental scaling law for PS-PMA micelles in mixed solvent 1,4-dioxane–water[15]. The pertinent micellar model applies to micelles, formed both by PS-PMA copolymer with dissociable PMA segments, and to those formed by PS-N-PMA-A copolymer in the case of hydrophobically tagged micelles. Since the micelles formed by symmetrical copolymers, i.e., by copolymer with comparable lengths of both blocks, are on average spherical nanoobjects, we perform simulations on a spherical lattice (Fig. 1). All lattice sites unoccupied by copolymer segments are occupied by solvent components, H_2O, H_3O^+, OH^-, Na^+, and Cl^-. By setting the concentration of H_3O^+, we adjust pH and by setting the concentration of Na^+ and Cl^-, the ionic strength of the solvent. To ensure that the numerical solution corresponds to a micelle centered in the origin of the spherical system of coordinates, we restricted the possible occurrence of PS segments only in the sphere with the radius 1.5 times larger than the estimated radius of the micellar core. Because we use SCF calculations for lattice, where the chain flexibility differs from that of real chains, the numbers of PS and PMA monomeric units in the chain and their sizes must be rescaled. The used lattice constants, effective numbers of segments and the Flory–Huggins interaction parameters χ(PS-solvent), χ(PMA-solvent) and χ(PS-PMA) used in calculation, were set by fitting experimental dimensions of micellar shell[15]. Here the solvent means an effective solvent containing

all non-polymer components of the system, H_2O, H_3O^+, OH^-, Na^+, Cl^-, and PMA means both, dissociated and nondissociated forms of PMA. Unfortunately, available experimental data do not allow for full parametrization (i.e., for settings such an extensive number of parameters). Therefore we had to reduce the number of parameters by using the following approximation. The micellar core is well segregated from the micellar shell and from the solvent, i.e., there exists a very narrow interface. To ensure the required segregation of PS from PMA and solvent, the interaction parameter between hydrophobic PS and the water solvent was set to a high value χ(PS-solvent) = 5.0. The lattice constant of PS was set equal to the lattice constant of PMA, $l = l_{PS} = l_{PMA}$, and the aggregation number, $N_{agg} = 113$, was calculated from the above mentioned empirical law. Using these fixed parameters we obtained the optimized parameters corresponding to the experimentally studied system PS-PMA ($M_w = 53000$, $w_{PS} = 0.52$, where M_w is weight-averaged molar mass, and w_{PS} weight fraction of PS)[16], $l = 1$ nm and χ(PMA-solvent) = 0.5. Because the shell dimension was only slightly dependent on the interaction parameter between PS and PMA, we set χ(PS-PMA) = 0. The number of segments of PS block, $N_{PS} = 75$, was calculated to reproduce the dimension of micellar core that, due to the strong segregation of core and shell, was estimated from the core density which matches the density of PS in amorphous state, 1.05 g cm^{-3}. The number of segments of PMA block, $N_{PMA} = 64$, was calculated from the contour length of the PMA part of a real chain and the lattice constant. For further details

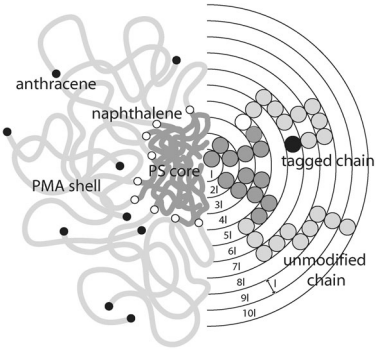

FIG. 1
The left-hand side: scheme of PS-N-PMA-A micelles in aqueous media. The right-hand side: SCF model of PS-PMA (unmodified) and PS-N-PMA-A (tagged) chain. PS segments are dark grey, PMA segments light grey, naphthalene white, and anthracene black. Lattice layers are labeled by multiples of lattice constant l

of the parametrization procedure, see ref.[17] For naphthalene between the PS and PMA blocks and anthracene at the ends of PMA blocks of the hydrophobically modified system, we used the same interaction parameters as for PS.

The knowledge of the structure of micelles formed by tagged PS-N-PMA-A chains, particularly the knowledge of distributions of naphthalene and anthracene tags allows to calculate the NRET efficiency, σ, between the donors of excitation energy, naphthalene, and the acceptors, anthracene. However, one more parameter has to be considered, i.e., the Förster radius, R_0, for the direct energy transfer from the donor to the acceptor[18]. Because there is no theoretical background on whether this NRET characteristics should be rescaled in lattice calculations and how, we simply use the literature value for naphthalene–anthracene pair, R_0 = 2.1 nm [19]. Moreover, we are aware that by using the lattice calculation, we introduce other inaccuracy in the calculated fluorescence behavior. It consists in the fact that the nearest possible distance between fluorophores is limited by the lattice constant and therefore the rate and probability of the energy transfer are limited; (l/R_0) (ref.[6]) is the upper limit of the transfer rate. Hence the Förster radius must be sufficiently large as compared with the lattice constant in order to prevent an underestimation of NRET effect. Nevertheless, we believe that in our case it does not affect considerably general trends and that theoretical and experimental data are comparable at a reasonable semiquantitative level. For calculation of the excitation energy transfer, we assume that under current conditions used in fluorometric measurements, one donor per micelle is excited at the maximum. Using the SCF method, which yields the angularly-averaged, i.e., only radially-dependent, probability of finding an acceptor in the distance r_{DA} from the excited donor, $\rho_{DA}(r_{DA})$, the NRET efficiency can be expressed by

$$\sigma = \frac{R_0^6 \int_0^{R_{eff}} \frac{\rho_{DA}(r_{DA})}{r_{DA}^6} \mathrm{d}r}{R_0^6 \int_0^{R_{eff}} \frac{\rho_{DA}(r_{DA})}{r_{DA}^6} \mathrm{d}r + \frac{1}{N_T}} \qquad (1)$$

where R_{eff} is the radius of effective sphere that contains all N_T traps to which the transfer can occur[20].

RESULTS AND DISCUSSION

The size of micelles is the most frequently measured and theoretically calculated property of micelles. From the experimental point of view, it is common to measure the hydrodynamic radius, R_h, by QELS. Unfortunately, the theoretical model for calculating R_h is fairly complex since it requires to treat hydrodynamic interactions and it is more common to calculate the radius of gyration, R_g. Both properties are proportional but the constant of proportionality depends on the inner structure of micelles[15]. For this reason we do not compare the measured and calculated values quantitatively and present a semiquantitative comparison only. The theoretically calculated radii of gyrations of shells of PS-PMA and PS-N-PMA-A micelles are shown in Fig. 2 as functions of pH for several ionic strengths, *I*, 0.1, 0.01, 0.001. The radius of gyration, R_g, increases steeply at pH higher than 5 and at pH 7 reaches a plateau. The height of the plateau (and also the height of the inflection point) decreases with increasing *I*. Radii of gyration of micelles formed by hydrophobically modified chains PS-N-PMA-A are almost the same as those of PS-PMA micelles, nevertheless, they are slightly lower at low pH and low *I*. The calculated data are in a reasonable agreement with those measured experimentally[16].

Figure 3 provides detailed view on R_g vs ionic strength dependence. It clearly indicates the non-monotonic dependence of R_g on *I*, $pI = -\log_{10} I$, in the region of medium pH. At pH > 7, R_g does not almost depend on pH, i.e., all measured values equal roughly to that for pH 7; however, it increases

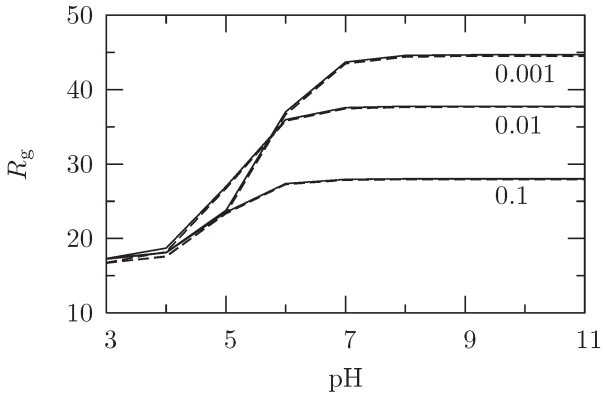

FIG. 2
The dependence of radius of gyration, R_g, of micellar shell on pH and ionic strength, *I*, for PS-PMA (solid curves) and PS-N-PMA-A (dashed curves) micelles. The curves are labeled by relevant values of *I*

monotonically with decreasing *I*. Figure 4 shows the probability density functions of nondissociated, ρ(PMAH), and dissociated, ρ(PMA⁻), PMA segments. The probability density function is defined as the probability of finding a nondissociated, or dissociated, PMA segment in a given distance from the center of micelle, which can be expressed by relations

$$\rho_z(\mathrm{PMAH}) = \frac{n_z(\mathrm{PMAH})}{\sum_z n_z(\mathrm{PMAH}) + n_z(\mathrm{PMA^-})} \tag{2}$$

and

$$\rho_z(\mathrm{PMA^-}) = \frac{n_z(\mathrm{PMA^-})}{\sum_z n_z(\mathrm{PMAH}) + n_z(\mathrm{PMA^-})} \tag{3}$$

where n_z(PMAH) and n_z(PMA⁻) are respectively the numbers of segments of nondissociated and dissociated PMA in layer *z*. In the inserts in Fig. 4, relevant degrees of dissociation of PMA segments are shown. At low pH, the segments of PMA are only little dissociated and neither the total dissociation nor the shell structure depend on *I*. At pH ≥ 7, the degree of dissociation approaches 1 and the structure of the shell depends only on ionic strength. It changes from the stretched brush structure at low *I* to the collapsed brush structure at high *I* due to the electrostatic screening of the repulsion between negatively charged PMA units by excess of small ions. In

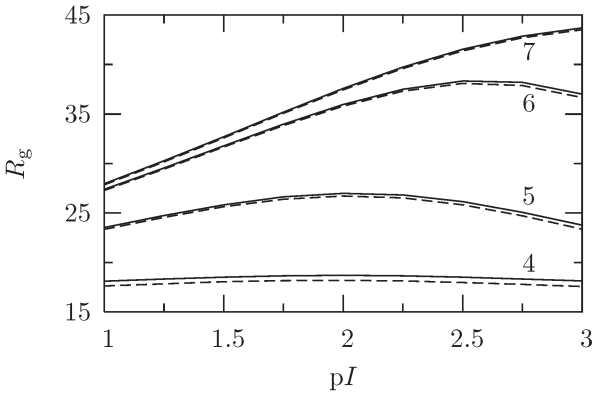

FIG. 3

The dependence of radius of gyration, R_g, of micellar shell on p*I* and pH for PS-PMA (solid curves) and PS-N-PMA-A (dashed curves) micelles. The curves are labeled by relevant pH values

the range of medium pH, the structure of micellar shells and the dissociation of PMA segments depend strongly on both pH and *I*. The dependence on *I* is very pronounced and quite interesting. At low *I* only few PMA at the micellar periphery are dissociated. The nondissociated PMA segments are localized relatively close to the core. The overall structure is fairly compact,

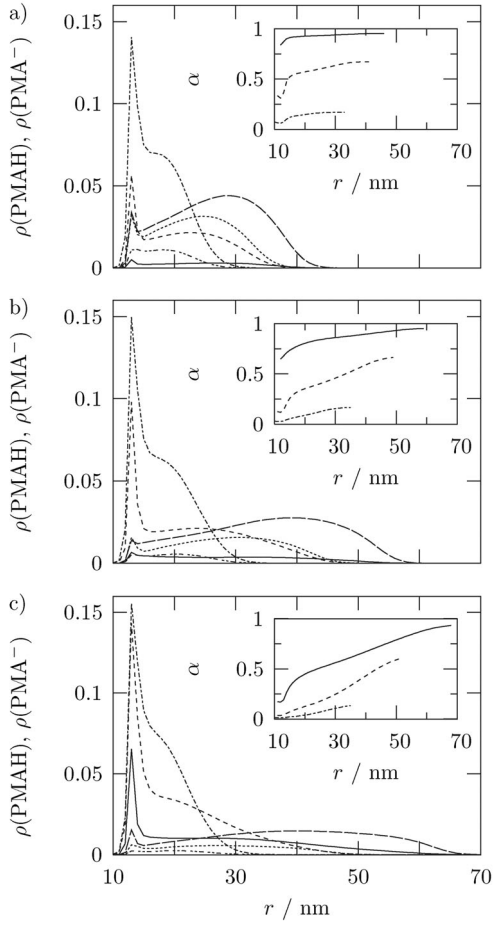

FIG. 4

Probability function of finding nondissociated and dissociated PMA segments in the distance *r* from the center of micelle. Figures a, b and c correspond to I = 0.1, 0.01 and 0.001, respectively. Different types of lines reflect different segments and pH values: nondissociated PMA at pH 6 (——), at pH 5 (– – –), at pH 4 (· – ·) and dissociated PMA at pH 6 (— —), at pH 5 (· · ·), at pH 4 (· · –). Inserts: degrees of dissociation of PMA segments. The same types of lines are used

except a thin peripheral layer. The degree of dissociation increases towards the shell periphery and, as already mentioned, increasing concentration of mutually repulsive PMA anions in PMA chains causes a considerable stretching of parts of PMA chains at the periphery of micelles. With increasing *I*, the dissociation increases but the electrostatic screening due to increasing concentration of counter-ions causes a collapse of PMA chains. For this reason, the radius of gyration, R_g, of the shell does not depend monotonically on *I* in the region of medium pH. The shell of micelles formed by hydrophobically modified PS-N-PMA-A copolymer behaves as the shell of non-modified micelles. Small differences are observed only at low pH where the dissociation of PMA segments is very low and occurs at the shell periphery only.

An interesting behavior of PS-PMA micelles can be observed at low *I* and pH below p*K*. The shell-forming PMA chains can be considered as an annealed brush densely grafted to a convex surface. Due to the spheric symmetry of micelles, the concentration of PMA decreases from the core/shell interface to the shell periphery, where the PMA chains are rather dilute. Although a major part of PMA is localized close to the core and is not dissociated, the peripheral part of PMA shell is significantly ionized. On one hand, the electrostatic attraction forces the counter-ions to remain in the shell and to compensate the negative charge of the shell. On the other hand, the osmotic pressure causes the escape of counter-ions from the shell. Due to the fairly low concentration of negative charges in the shell and their large distances, the electrostatic interactions do not prevent an important fraction of small ions from escaping to the bulk solvent. In Fig. 5

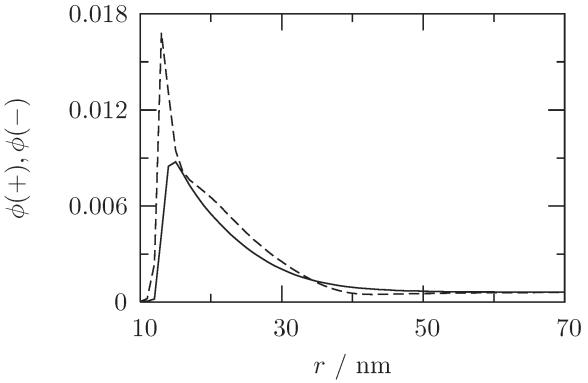

FIG. 5
Density of charges as a function of the distance from the center of micelle for pH 4.6 and I = 0.001. The solid curve shows positive charges, dashed curve negative charges

the densities of positive, $\phi(+)$, and negative, $\phi(-)$, charges (the ratios of numbers of charges and number of lattice sites in a given layer) are shown. It is seen that the negative charges of PMA shell are not fully compensated by counter-ions and a broad electric double layer is formed. In this respect, the shell-forming PMA chains at low pH and low I resemble the polyelectrolyte Pincus brush[21]. This has been proven also by recent experimental studies in solutions with very low I. With increasing I, the behavior of PMA shell changes from the Pincus brush to the salted brush.

The behavior of the shell of PS-PMA micelles and PS-N-PMA-A micelles differs mainly at low pH and low I, where the dissociation of PMA segments is low and the dimensions of the shell are not driven by electrostatic forces.

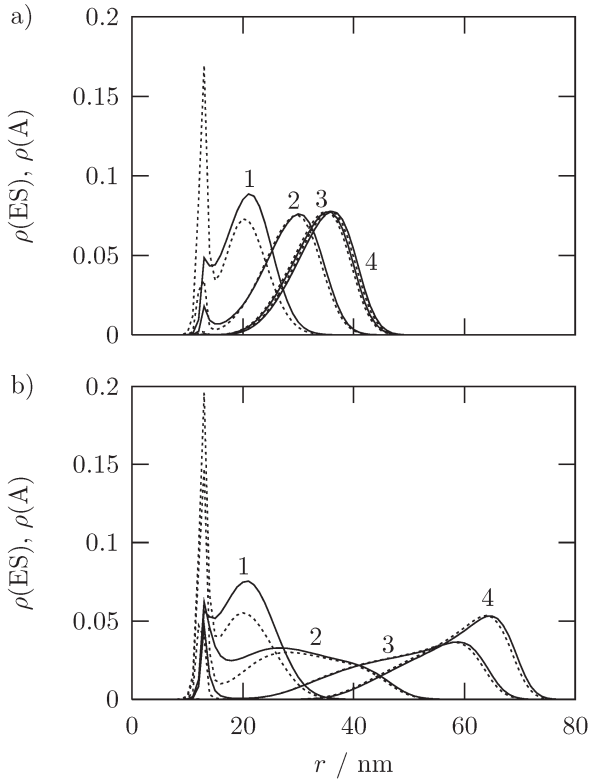

FIG. 6

Probability density function of finding end segments of PMA chains (ES) of non-modified PS-PMA micelles (solid lines) and anthracene (A) of hydrophobically modified PS-N-PMA-A micelles (dashed lines) in the distance r from the center of micelle, I = 0.001 (a) and I = 0.1 (b), curves *1*, *2*, *3* and *4* correspond to pH 4, 5, 6 and 7, respectively

Under these conditions, different hydrophobicity of the end methacrylic acid unit in the case of PS-PMA micelles, and anthracene in the case of PS-N-PMA-A micelles, plays an important role in the shell behavior and affects the shell structure. Due to the unfavorable anthracene–water interaction, a part of PMA chains loops back to the less polar environment close to the core/shell interface. With increasing pH and *I*, the differences vanish and the shells of both types of micelles behave similarly. The probability density functions of finding the end segment (either the methacrylic acid unit or anthracene) in the distance *r* from the micelle center for different pH and *I* are shown in Fig. 6. Small peaks of the end methacrylic acid segments of PS-PMA micelles at the core/shell interface are caused by a more favorable short-range interaction between PMA and the core-forming PS than between PMA and the solvent.

In the last part of the paper, the nonradiative excitation energy transfer from naphthalene in the interface to anthracene attached at the ends of PMA blocks was calculated. In Fig. 7, the experimentally measured and theoretically calculated NRET efficiencies, σ, are shown. The calculated values of σ were obtained from Eq. (*1*), on the basis of the distribution of donor-to-acceptor distances, which were recalculated from the SCF-obtained radial distribution functions by a simple Monte Carlo sampling method. The experimental and calculated data are in a reasonable agreement in the whole pH range. At pH 5–7, the calculated σ are lower than the experimental values, which is due to approximations involved in the model and, more im-

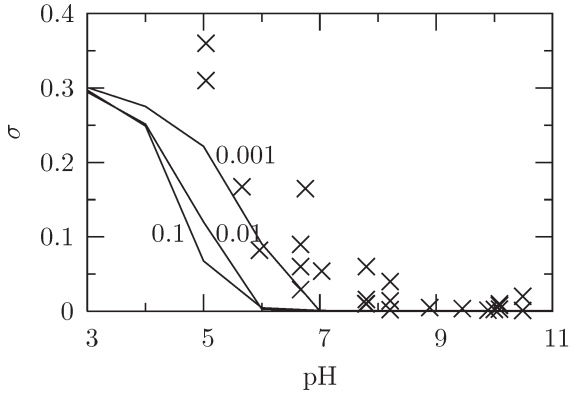

FIG. 7
The dependence of NRET efficiency, σ, on pH for different values of *I* for PS-N-PMA-A micelles. Calculated curves are labeled by relevant *I* values. Data from experimental measurements at *I* changing from 0.01 to 0.1 are displayed as crosses

portantly, due to the fact that the p*K* dependence of PMA on the degree of dissociation was neglected. The dissociation constant of weak polyelectrolytes depends considerably on the degree of dissociation. In the case of PMA, p*K* increases more than three units in the range from $\alpha = 0.46$ to $\alpha = 0.8$ (ref.[22]). Since in most calculations of other authors[23,24] constant values of p*K* were used, we used the same approximation as the first rough estimate to get the most decisive features of the behavior. The change of p*K* with α will be taken into account in future studies. The unavailability of experimental values of σ at pH ≤ 4 is due to the low solubility of nondissociated PMA in water and, consequently, instability of micellar systems. Despite the differences between experimentally measured and theoretically calculated values, basic trends are in a good agreement and the used model describes the experimentally observed behavior quite well.

The authors thank the Grant Agency of the Czech Republic (grants Nos 203/03/0262, 204/04/P117 and 203/04/0490) for financial support and the MetaCenter project of the CESNET for computer time. This work was supported by the EU within Marie Curie Research and Training Network (grant No. 505027, POLYAMPHI).

REFERENCES

1. Tuzar Z., Kratochvíl P. in: *Surface and Colloid Science* (E. Matijević, Ed.), Vol. 15. Plenum Press, New York 1993.
2. Astafieva I., Khougaz K., Eisenberg A.: *Macromolecules* **1995**, *28*, 7127.
3. Khougaz K., Astafieva I., Eisenberg A.: *Macromolecules* **1995**, *28*, 7135.
4. Antonietti M., Forster S., Oestreich S.: *Macromol. Symp.* **1997**, *121*, 75.
5. Kakizawa Y., Kataoka K.: *Adv. Drug Delivery Rev.* **2002**, *54*, 203.
6. Kataoka K., Harada A., Nagasaki Y.: *Adv. Drug Delivery Rev.* **2001**, *47*, 113.
7. Kwon G. S., Kataoka K.: *Adv. Drug Delivery Rev.* **1995**, *16*, 295.
8. van Nostrum C. F.: *Adv. Drug Delivery Rev.* **2004**, *56*, 9.
9. Hennink W. E., van Nostrum C. F.: *Adv. Drug Delivery Rev.* **2002**, *54*, 13.
10. Uhlík F., Limpouchová Z., Jelínek K., Procházka K.: *J. Chem. Phys.* **2004**, *121*, 2367.
11. Fleer G. J., Cohen Stuart M. A., Scheutjens J. M. H. M., Cosgrove T., Vincent B.: *Polymers at Interfaces*, Chap. 4. Chapman & Hall, London 1993.
12. Böhmer M. R., Evers O. A., Scheutjens J. M. H. M.: *Macromolecules* **1990**, *23*, 2288.
13. Israëls R., Leermakers F. A. M., Fleer G. J.: *Macromolecules* **1994**, *27*, 3087.
14. Jelínek K., Uhlík F., Limpouchová Z., Procházka K.: *J. Phys. Chem. B* **2003**, *107*, 8241.
15. Qin A., Tian M., Ramireddy C., Webber S. E., Munk P., Tuzar Z.: *Macromolecules* **1994**, *27*, 120.
16. Karymov, M. A., Procházka K., Mendenhall J. M., Martin T. J., Munk P., Webber S. E.: *Langmuir* **1996**, *12*, 4748.
17. Uhlík F., Limpouchová Z., Jelínek K., Procházka K.: *J. Chem. Phys.* **2003**, *118*, 11258.
18. Förster T.: *Z. Naturforsch., A* **1949**, *4*, 321.

19. Berleman I. B.: *Energy Transfer Parameters of Aromatic Compounds*. Academic Press, New York, London 1973.
20. Mendelsohn A. S., Delacruz M. O., Torkelson J. M.: *Macromolecules* **1993**, *26*, 6789.
21. Pincus P.: *Macromolecules* **1991**, *24*, 2912.
22. Porasso R. D., Benegas J. C., van den Hoop M. G. T.: *J. Phys. Chem.* **1999**, *103*, 2361.
23. Zhulina E. B., Birshtein T. M., Borisov O. V.: *Macromolecules* **1995**, *28*, 1491.
24. Zhulina E. B., Borisov O. V.: *Macromolecules* **2002**, *35*, 9191.